



Directional magnetoelectric effect in multi-electrode Pb(Zr,Ti)O₃/Ni cylindrical layered composite



Lirong Xu^a, De'an Pan^{a,*}, Lijie Qiao^a, Alex A. Volinsky^b, Yang Song^a

^a Institute of Advanced Materials and Technology, University of Science and Technology Beijing, Beijing 100083, China

^b Department of Mechanical Engineering, University of South Florida, Tampa, FL 33620, USA

ARTICLE INFO

Article history:

Received 4 June 2015

Received in revised form 27 September 2015

Accepted 28 September 2015

Available online 30 September 2015

Keywords:

Magnetoelectric effect

Multi-electrode

Directionality

Extensional mode

ABSTRACT

Directional magnetoelectric (ME) effect was found in multi-electrode PZT/Ni cylindrical layered ME composite with external magnetic field applied perpendicular to the cylinder axis. The composite with the radially polarized PZT ring was electroplated with four Ni arc layers. Both the ME voltage coefficient and the corresponding phase suggest that the ME effect is omni-directional around the fundamental extensional mode of the PZT ring and directional around the third extensional mode with different magnetic field orientation. ME sensor with this compact structure can be used to determine the magnetic field orientation by measuring the ME voltage amplitude and the corresponding phase.

© 2015 Elsevier Ltd. All rights reserved.

1. Introduction

Magnetoelectric (ME) effect is defined as the influence of magnetic (electric) field on the polarization (magnetization) of a material. In a composite consisting of magnetostrictive and piezoelectric phases, the ME effect is a product property [1]. Multi-phase ME composites exhibit giant ME effect at room temperature with great design flexibility, which is lacking in single phase ME materials. Laminated ME composites show the strongest ME effect and have been extensively studied, having promising applications in sensors, phase shifters, transducers, filters and so on [2–7]. In such laminates the ME coupling is realized by the strain transfer across the interface between the piezoelectric and magnetostrictive phases. Therefore, laminate vibration modes and corresponding strain distribution determine the ME effect [8]. ME laminates with different shapes and configurations have been made. They have different vibration modes, such as bending and radial vibration in disk laminates [9], bending and longitudinal vibration in rectangular composites and torsion vibration in other structures [10–13]. It has been demonstrated that Ni/PZT and Ni/PZT/Ni cylindrical ME laminates made by electroplating have giant ME coupling with radial and axial vibration modes [14,15]. Since ME laminate vibrations are induced by the applied magnetic field, the ME effect is influenced by both the direction and the strength of the magnetic field. For ME laminates applications, especially in magnetic field sensors, the field-direction-dependent ME effect is crucial to treat uncertain magnetic field vector. A few studies have reported anisotropic ME effects in response to

magnetic field direction. ME anisotropy results from the piezoelectric, magnetostrictive and/or shape anisotropy [16–19]. However, the investigated ME coefficients are averaged over the whole surface of piezoelectric layer and only a few studies have considered anisotropic ME effects at different positions of the piezoelectric layer.

Moreover, the ME coefficient has been proven to be a complex quantity, resulting from the ME loss, which includes electromechanical, magneto-mechanical and interfacial losses between the piezoelectric and magnetostrictive layers [8,12,20,21]. The phase delay of the ME voltage output with respect to externally applied magnetic field originates from the energy transfer efficiency loss in ME composites. Thus, the ME coefficient phase also reflects the ME characteristics.

In this work the ME voltage coefficient and the corresponding phase of the multi-electrode Pb(Zr,Ti)O₃/Ni cylindrical composite in the vertical mode were investigated. The structure consists of an intact PZT ring and four Ni arcs on the inside PZT surfaces. Various vibration modes result in the ME effects of the four arcs having different relationship with the applied magnetic field orientation. The ME coefficient phase showed directionality in high order vibration modes, which is helpful to design ME sensors.

2. Experimental

The multi-electrode Pb(Zr,Ti)O₃/Ni cylindrical layered composite, shown schematically in Fig. 1, was prepared by electroplating. The PZT-5H ceramic ring with the dimensions of $\Phi 25 \times \Phi 23 \times 10$ mm³ was radially polarized. The Ni electrodes on both the inside and outside PZT ring surfaces were equally spaced. They were separated by narrow gaps along the cylinder axis to electrically isolate the electrodes. Four Ni

* Corresponding author.

E-mail address: pandean@mater.ustb.edu.cn (D. Pan).

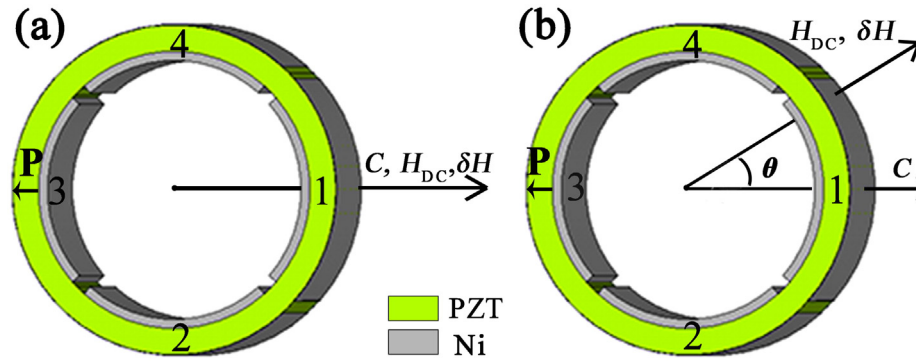


Fig. 1. Schematic illustration of the multi-electrode Pb(Zr,Ti)₃O/Ni ring with arrayed Ni arc layers under external magnetic field H applied along: (a) the perpendicular bisector C of the unit 1 ($\theta = 0^\circ$); (b) an angle θ with respect to C . θ denotes the angle between H and C .

arc layers were electroplated on the inner electrodes simultaneously. The final magnetostrictive Ni thickness was approximately 340 μm . The Ni electroplating bath composition and conditions are described elsewhere [14]. Four ME measurement units (units 1, 2, 3 and 4) are labeled in Fig. 1a. The ME characterization was performed in the ME measurement system, where a DC bias magnetic field (H_{DC}) superimposed with a collinear alternating (δH) magnetic field was applied perpendicular to the cylinder axis (vertical mode). Considering the non-rotational symmetry of the composite, two different measurements were performed with the external magnetic field H applied along the perpendicular bisector C of unit 1 and at an angle θ with respect to C , as shown in Fig. 1b. The ME voltage coefficient was calculated as $\alpha_{\text{E,V}} = \delta V / (t_{\text{PZT}} \cdot \delta H)$, where t_{PZT} is the PZT thickness and δH is the amplitude of the AC magnetic field generated by the Helmholtz coils. The phase φ between the output ME voltage and the sinusoidal AC magnetic field δH were recorded simultaneously.

3. Results and discussion

Fig. 2a shows the external magnetic field frequency dependence of $\alpha_{\text{E,V}}$ and φ for the unit 1 within the 1 kHz to 120 kHz range, while Fig. 2b shows the frequency dependence of $\alpha_{\text{E,V}}$ and φ for each of the four units at two resonance regions when $\theta = 0^\circ$. The DC bias magnetic field $H_{\text{DC}} = 110$ Oe was applied during all measurements. For units 2, 3 and 4, there are two resonance peaks for the ME voltage coefficient, similar to the unit 1. There is a significant phase shift around each resonance frequency. In previous report of the axial mode, two resonance $\alpha_{\text{E,A}}$ peaks of each unit appear at 42 kHz and 59.3 kHz [22]. Here in the vertical mode, the two peaks appear at 42 kHz and 93.7 kHz. The resonance $\alpha_{\text{E,A}}$ peaks are near electromechanical anti-resonance frequency (f_a) of the piezoelectric layer [23]. Note that f_a of the radial vibration mode was provided by the manufacturer for the PZT ring as 38.5 kHz. It is quite likely that the first $\alpha_{\text{E,A}}$ peak at 42 kHz is associated with the radial

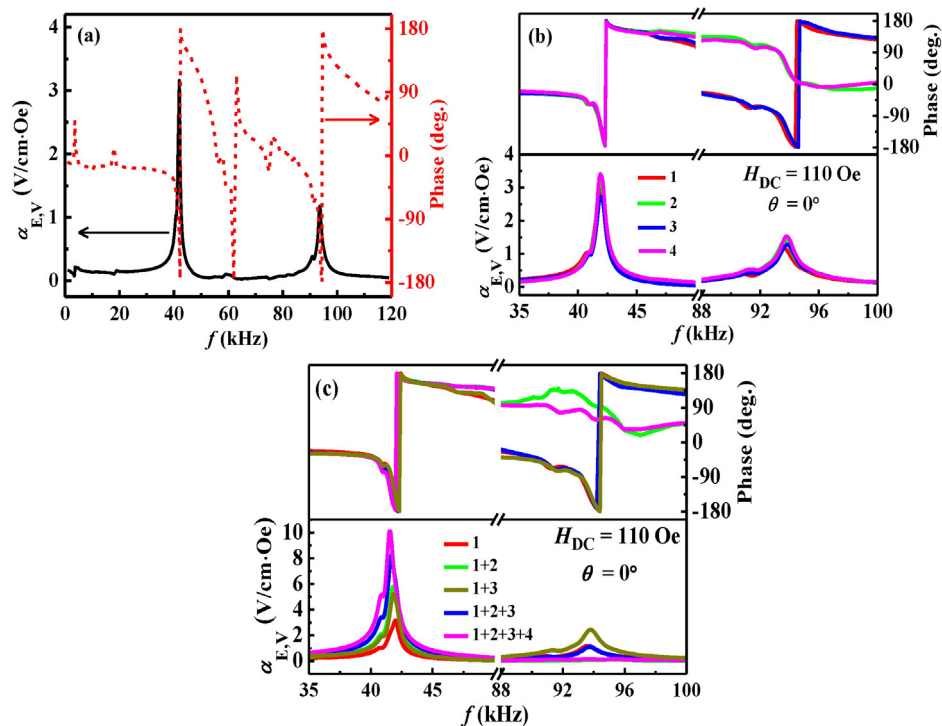


Fig. 2. Frequency dependence of the ME voltage coefficient $\alpha_{\text{E,V}}$ and the phase φ for: (a) unit 1 from 1 kHz to 120 kHz; (b) units 1–4 and (c) the four units connected in series sequentially around the resonance regions with $H_{\text{DC}} = 110$ Oe and $\theta = 0^\circ$.

extensional vibration mode of the composite. The three resonance frequencies of 42 kHz, 59.3 kHz and 93.7 kHz are related. In fact, the two higher frequencies have the following relations with the lowest frequency: $59.3 \text{ kHz}/42 \text{ kHz} \approx \sqrt{2}$ and $93.7 \text{ kHz}/42 \text{ kHz} \approx \sqrt{5}$. Moreover, for a short and thin-walled ring, the n^{th} extensional mode has a resonance frequency of $f_n = f_0 \sqrt{1 + n^2}$, where f_0 is the resonance frequency of the fundamental extensional mode with the mode number $n = 0$ [24, 25]. Based on this, the first peak at 42 kHz corresponds to the fundamental extensional mode, while the second peak in the vertical mode corresponds to the third extensional mode with $n = 2$.

As seen in Fig. 2b on the expanded frequency scale, the four units at the two peaks have almost the same ME voltage coefficients $\alpha_{E,V}$ and the curves almost overlap with each other. For all resonance peaks, the phase shifts are all nearly 180° , consistent with previous reports [9, 12]. The curves for the phase φ around the first peaks also coincide. However, it is not the case around the second peaks, i.e. the curves are divided into two superimposed groups. The two groups are units 1 and 3, and units 2 and 4, while the phase difference between them is close to 180° . Since the ME effect is related to the vibration modes and the corresponding strain distribution, the ME voltage shows the same symmetry with the strain of the piezoelectric layer, especially at the resonance frequencies [26]. Then the $\alpha_{E,V}$ phase depends on the phase of the PZT ring strain. When the PZT ring vibrates in the fundamental extensional mode, the radial extensional strain is in phase at all circumferential locations. Therefore, the ME effect is omni-directional in the whole PZT ring and the four units exhibit equivalent ME effect with almost the same $\alpha_{E,V}$ and φ at the first peak. In the case of $\theta = 0^\circ$, the magnetostrictive strain strongly depends on the change of the magnetization component perpendicular to the sensing field [27]. The strain transferred to the piezoelectric phase of units 1 and 3 differs from that of units 2 and 4 as a result of different magnetization in the Ni layers. Similar to the electric field voltage distribution exciting the third extensional mode of the piezoelectric ceramic ring [24,25], the third extensional mode of the PZT ring can be activated. Since the ring vibrates in the third extensional mode, there are four longitudinal nodal lines with zero displacement. Radial strain is harmonic in the azimuth angle in the horizontal plane perpendicular to the cylinder axis. Thus, the ME effect is periodic with respect to the angle, and the opposite units have equivalent ME effect, while the adjacent units have equal amplitude, but inverse phase ME effect at the second peak.

To further investigate the relevance of the ME effect in different units, the four units were electrically connected in series sequentially, as shown in Fig. 2c. Around the first peak, $\alpha_{E,A}$ increases multiplicatively, while φ for all connections shares the same characteristics. It confirms that at the first peak the ME effect is circumferentially uniform due to the fundamental radial extensional mode. This means that the electrodes can be divided further as proposed in this paper. Arc electrodes on a single PZT ring connected in series can improve the ME voltage output of the compact structure. Not surprisingly, both $\alpha_{E,V}$ and φ vary for different connection types around the second peak. When the opposite units 1 and 3 are connected in series, $\alpha_{E,A}$ increases nearly twice due to the similar phases of the two units. The peaks of $\alpha_{E,A}$ disappear for units 1 and 2 connected in series and for the four units connected in series, while $\alpha_{E,A}$ remains the same as unit 1 for units 1, 2 and 3 connected in series. Meanwhile, φ for the units 1, 2 and 3, and units 1 and 3 connected in series overlap with the unit 1. The phase shifts for the units 1 and 2 connected in series and all the four units connected in series are approximately 90° rather than 180° . This indicates that the ME voltages of the adjacent units around the second resonance mode will cancel each other when connected in series. Less than 180° phase shift shows that there is still ME loss, since vibration does not vanish with different circuit connections. It is worth noting that the inverse phases reflect the magnetic field orientation.

The $\alpha_{E,V}$ and φ frequency dependence with $H_{DC} = 110 \text{ Oe}$ is presented in Fig. 3 for various θ angles of the magnetic field H with respect

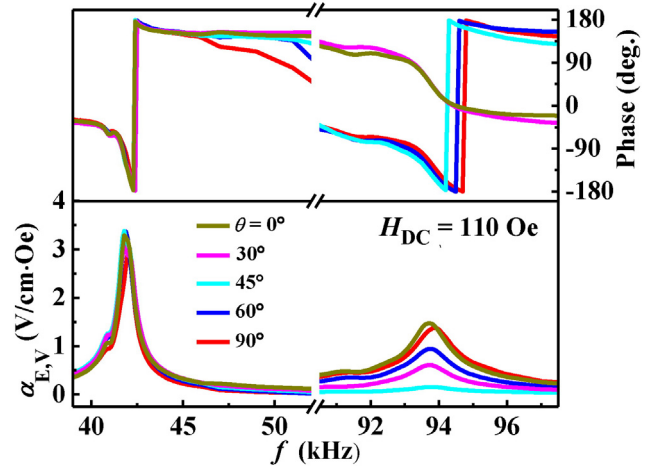


Fig. 3. Unit 1 frequency dependence of the ME voltage coefficient $\alpha_{E,V}$ and the phase φ for $\theta = 0^\circ, 30^\circ, 45^\circ, 60^\circ$, and 90° with $H_{DC} = 110 \text{ Oe}$.

to the perpendicular bisector C of the unit 1. At the first peak, both $\alpha_{E,V}$ and φ for different θ share almost the same characteristics as different units with $\theta = 0^\circ$, as discussed previously. Thus, the ME effect around the fundamental extensional mode of the PZT ring has no dependence on the magnetic field orientation. This is mainly due to the total effective magnetization of the four units barely changing during the ring rotation. At the second resonance peak, the maximum $\alpha_{E,V}$ decreases until $\theta = 45^\circ$ and then increases as θ changes from that for $\theta = 0^\circ$ to 90° , while the phase shifts are all near 180° . The $\alpha_{E,V}$ almost vanishes at $\theta = 45^\circ$, since the strain transferred to the PZT ring is equivalent in the four units and the third extensional mode cannot be excited. The maximum $\alpha_{E,V}$ for $\theta = 30^\circ$ and 60° is smaller than that for $\theta = 0^\circ$ and 90° , since the gaps between the electrodes cause somewhat different strain transferred to the PZT ring, and a small component of the third extensional mode can be excited. Actually, the vanishing $\alpha_{E,V}$ peak with nearly 180° phase shift of the unit 1 around 59.3 kHz in Fig. 1a indicates that the second extensional vibration mode is not excited in the vertical mode. For $\theta = 0^\circ$ or 90° , the strain difference reaches the maximum and the third extensional mode can be fully excited, so the $\alpha_{E,V}$ is the highest. The curves of φ also vary with increasing θ . The phase difference is small between $\theta = 0^\circ$ and 30° . However, the phase changes nearly 180° when θ increases to $45^\circ, 60^\circ$ and 90° . The shifts between the three curves are evident in Fig. 3. Hence, the ME effect for the unit 1 shows directionality with the magnetic field in terms of both $\alpha_{E,V}$ and the phase around the third extensional mode. By measuring both $\alpha_{E,V}$ and φ of the four units around the third extensional mode, the orientation of the magnetic field can be determined. With further research into the dependence of the ME effect on the angle between the external AC and DC magnetic fields, one could design a single-axis magnetic field sensor. For spatial magnetic field detection, one could integrate a three-axis sensor unit, where the sensors are orthogonal to each other [11].

4. Conclusions

Multi-electrode PZT/Ni cylindrical layered ME composite was electroplated with four Ni arc layers on the radially polarized PZT ring. The vertical ME measurements of both the ME voltage coefficient and the corresponding phase show that the ME effect is omni-directional around the fundamental extensional mode of the PZT ring and directional around the third extensional mode with different magnetic field orientation. The directionality in both the amplitude and the phase of the ME voltage is helpful to determine the direction of the magnetic field in the ME sensor using this compact ME composite structure.

Acknowledgments

This work was supported by the Beijing Nova Program (Z141103001814006), by the National Natural Science Foundation of China (51472030, 51174247 and U1360202), by the Fundamental Research Funds for the Central Universities (Project No: FRF-TP-14-001C1), the China Postdoctoral Science Foundation Funded Project (Project No: 2014M560885) and by the National Science Foundation (IRES1358088).

References

- [1] W. Eerenstein, N.D. Mathur, J.F. Scott, Multiferroic and magnetoelectric materials, *Nature* 442 (2006) 759–765.
- [2] G. Srinivasan, Magnetoelectric composites, *Annual Review of Materials Research* 40 (2010) 153–178.
- [3] J. Ma, J. Hu, Z. Li, C.W. Nan, Recent progress in multiferroic magnetoelectric composites: from bulk to thin films, *Advanced Materials* 23 (2011) 1062–1087.
- [4] J. Zhai, Z. Xing, S. Dong, J. Li, D. Viehland, Magnetoelectric laminate composites: an overview, *Journal of the American Ceramic Society*, 91 (2008) 351–358.
- [5] C.-W. Nan, M.I. Bichurin, S. Dong, D. Viehland, G. Srinivasan, Multiferroic magnetoelectric composites: historical perspective, status, and future directions, *Journal of Applied Physics* 103 (2008) 031101.
- [6] Y. Wang, J. Li, D. Viehland, Magnetoelectrics for magnetic sensor applications: status, challenges and perspectives, *Materials Today* 17 (2014) 269–275.
- [7] P. Zachariasz, J. Kulawik, P. Guzdek, Preparation and characterization of the microstructure, dielectric and magnetoelectric properties of multiferroic $\text{Sr}_3\text{CuNb}_2\text{O}_9\text{-CoFe}_2\text{O}_4$ ceramics, *Materials and Design* 86 (2015) 627–632.
- [8] J.-P. Zhou, Z.-C. Qiu, P. Liu, W.-C. Sun, H.-W. Zhang, Magnetoelectric resonant characteristics in $\text{Pb}(\text{Zr},\text{Ti})\text{O}_3/\text{Terfenol-D}$ laminate composites, *Journal of Applied Physics* 103 (2008) 103522.
- [9] Z. Shi, L. Chen, Y. Tong, H. Xue, S. Yang, C. Wang, et al., Giant phase shift effect in $\text{Tb}_{0.3}\text{Dy}_{0.7}\text{Fe}_2/\text{Pb}(\text{Zr},\text{Ti})\text{O}_3$ laminated composite, *Applied Physics Letters* 102 (2013) 112904.
- [10] L. Li, X.M. Chen, H.Y. Zhu, Unique dependence of magnetoelectric voltage coefficient on bias magnetic field in Terfenol-D/ $\text{Pb}(\text{Zr},\text{Ti})\text{O}_3$ bi-layered composites, *Journal of Alloys and Compounds* 553 (2013) 86–88.
- [11] X.W. Dong, B. Wang, K.F. Wang, J.G. Wan, J.M. Liu, Ultra-sensitive detection of magnetic field and its direction using bilayer PVDF/Metglas laminate, *Sensors and Actuators A: Physical* 153 (2009) 64–68.
- [12] J.-P. Zhou, Y.-J. Ma, G.-B. Zhang, X.-M. Chen, A uniform model for direct and converse magnetoelectric effect in laminated composite, *Applied Physics Letters*, 104 (2014) 202904.
- [13] J. Han, J. Hu, S.X. Wang, J. He, A novel cylindrical torsional magnetoelectric composite based on d_{15} shear-mode response, *Journal of Physics D: Applied Physics* 48 (2015) 045001.
- [14] D.A. Pan, Y. Bai, A.A. Volinsky, W.Y. Chu, L.J. Qiao, Giant magnetoelectric effect in Ni-lead zirconium titanate cylindrical structure, *Applied Physics Letters*, 92 (2008) 052904.
- [15] D. Xie, Y.G. Wang, J.H. Cheng, Length dependence of the resonant magnetoelectric effect in $\text{Ni}/\text{Pb}(\text{Zr},\text{Ti})\text{O}_3/\text{Ni}$ long cylindrical composites, *Journal of Alloys and Compounds*, 615 (2014) 298–301.
- [16] S. Chen, X.F. Yang, J. Ouyang, G.Q. Lin, F. Jin, B. Tong, Fabrication and characterization of shape anisotropy $\text{AlN}/\text{FeCoSiB}$ magnetoelectric composite films, *Ceramics International*, 40 (2014) 3419–3423.
- [17] J.X. Ye, J.M. Hu, Z. Shi, Z. Li, Y. Shen, J. Ma, C.W. Nan, Magnetic-field-orientation dependent magnetoelectric effect in $\text{FeBSiC}/\text{PZT}/\text{FeBSiC}$ composites, *Advances in Materials Science and Engineering*, 249526 (2014) 1–5.
- [18] J.L. Jones, J.D. Starr, J.S. Andrew, Anisotropy in magnetoelectric composites, *Applied Physics Letters* 104 (2014) 242901.
- [19] P. Martins, A. Larrea, R. Gonçalves, G. Botelho, E.V. Ramana, S.K. Mendiratta, et al., Novel anisotropic magnetoelectric effect on $\delta\text{-FeO}(\text{OH})/\text{P}(\text{VDF-TrFE})$ multiferroic composites, *ACS Applied Materials & Interfaces*, 7 (2015) 11224–11229.
- [20] L. Li, S.Y. Wu, X.M. Chen, Y.Q. Lin, Frequency-dependent magnetoelectric coefficient in a magnetostrictive–piezoelectric composite as a complex quantity, *Journal of Physics D: Applied Physics* 41 (2008) 125004.
- [21] J. Zhai, J. Li, D. Viehland, M.I. Bichurin, Large magnetoelectric susceptibility: the fundamental property of piezoelectric and magnetostrictive laminated composites, *Journal of Applied Physics* 101 (2007) 014102.
- [22] L.R. Xu, D.A. Pan, Z.J. Zuo, J. Wang, A.A. Volinsky, L.J. Qiao, Multi-electrode $\text{Pb}(\text{Zr},\text{Ti})\text{O}_3/\text{Ni}$ cylindrical layered magnetoelectric composite, *Applied Physics Letters*, 106 (2015) 032904.
- [23] K.-H. Cho, Y. Yan, C. Folgar, S. Priya, Zigzag-shaped piezoelectric based high performance magnetoelectric laminate composite, *Applied Physics Letters*, 104 (2014) 222901.
- [24] A.E.H. Love, *Mathematical Theory of Elasticity*, 4th ed. Cambridge University Press, London, 1934 452.
- [25] J.L. Butler, A.L. Butler, J.A. Rice, A tri-modal directional transducer, *The Journal of the Acoustical Society of America*, 115 (2004) 658.
- [26] J.-P. Zhou, L. Meng, Z.-H. Xia, P. Liu, G. Liu, Inhomogeneous magnetoelectric coupling in $\text{Pb}(\text{Zr},\text{Ti})\text{O}_3/\text{Terfenol-D}$ laminate composite, *Applied Physics Letters*, 92 (2008) 062903.
- [27] N.O. Urs, I. Teliban, A. Piorra, R. Knöchel, E. Quandt, J. McCord, Origin of hysteretic magnetoelastic behavior in magnetoelectric 2–2 composites, *Applied Physics Letters*, 105 (2014) 202406.